

Subjective Likelihood *

Ana Grohovac Rappold

Michael Lavine

US EPA

Duke University

Susan Lozier

Duke University

May 25, 2005

1 Introduction

This paper describes a Bayesian statistical analysis using data without a sampling model and therefore without an obvious likelihood function. Our approach is to elicit the likelihood function directly from the expert. The problem arose in an analysis of ocean temperature data, in an attempt to

*supported by NSF grant #ATM-0221939

learn about long term changes in the ocean's climate.

The typical Bayesian analysis posits data from a parametric family of sampling distributions, as in Equation 1.

$$\vec{y} \sim p(\vec{y} | \theta) \tag{1}$$

After \vec{y} has been observed it is treated as fixed, and the likelihood function is defined to be $\ell(\theta) \equiv p(\vec{y} | \theta)$, a function of θ . The interpretation is that likelihood ratios $\ell(\theta_1)/\ell(\theta_2)$ quantify \vec{y} 's evidence for θ_1 as opposed to θ_2 .

For our data set there is no believable sampling model $p(\vec{y} | \theta)$, so we cannot assign $\ell(\theta) \equiv p(\vec{y} | \theta)$. We take a different approach, wherein lies the statistical novelty of this paper. For several values of i , about a dozen, we show the expert \vec{y}_i and directly elicit her posterior distribution $p(\theta | \vec{y}_i)$. Elicitation is done under conditions where the expert has an approximately uniform prior for θ . After elicitation we know the prior and posterior and can therefore infer the likelihood function.

After examining the dozen or so elicited posteriors and conferring with the expert, we constructed an algorithm that accepts a \vec{y} as input and yields a likelihood function $\ell(\theta)$ as output. After constructing the algorithm we checked that it gave sensible results on several hundred more \vec{y} 's. We call ℓ a likelihood function because it approximately summarizes the expert's weight

of evidence and, when multiplied by the uniform prior, yields her posterior. We then apply the algorithm to our full collection of data $\{\vec{y}_i\}_{i=1}^T$ which, when combined with our real prior, yields our posterior.

The data arise in a study of the ocean's climate. The situation is more complicated than described in this introduction, as the data are a time series and our model must account for an annual cycle. Section 2 describes the scientific background while Section 3 describes the data. Section 4 describes our subjective likelihood, how it was elicited, and how it is modelled. It contains whatever statistical novelty is in this paper. Section 5 describes our prior, accounting for the annual cycle, year-to-year variation, heteroscedasticity, and a possible secular trend. The posterior is found by MCMC; it is described in Section 6. Section 7 is a discussion and Section 8 is an appendix describing an alternative model that we ultimately rejected.

2 Oceanography

A major focus of recent environmental research has been the detection and analysis of anthropogenic impacts on global climate. According to present understanding, there is a discrepancy between the warming that has been

detected in the atmosphere and that which is expected to have occurred under mathematical models of the earth's energy budget. To resolve the mismatch climatologists look for changes in the climate of the ocean.

One way to look for changes in the ocean's climate is through temperature, as has been done by, among others, Roemmich and Wunsch [1984], Levitus [1989a], Levitus [1989b], Read and Gould [1992], Bindoff and McDougall [1994], Parrilla et al. [1994], and Lavine and Lozier [1999]. But that's just one way to monitor climate change; in this paper we use another. We examine a structural feature of the ocean, the *mixed layer*, to see whether its depth M has changed over time.

To a first approximation, oceanographers regard the ocean as having two layers: a mixed layer from the surface down to as much as several hundred meters, and a stratified layer beneath. Mixing in the upper layer is due primarily to wind, waves, and thermal convection. The depth M of the mixed layer evolves through an annual cycle and is a function of geographic location, atmospheric conditions, and the ocean's heat content. Thus, long term changes in heat content may result in long term changes in M .

The mixed layer is important biologically because production of plankton is tightly coupled to sunlight. Plankton in the mixed layer can easily rise to

the surface and be exposed to sunlight, whereas plankton below the mixed layer tend to gravitate to the ocean floor. The mixed layer is also physically important. The large scale flow of waters is governed by upwelling and downwelling where large water masses come together. In regions of downwelling, waters below the mixed layer descend under density differences. Oceanographers are concerned that permanent alterations in M can disturb both the kinetics and the biology of the ocean.

Our study of M and whether it has a secular trend, will aid in closing the earth's energy budget and will increase our understanding of potential physical and biological consequences of global warming.

3 Data

There are three main sources of data about the oceans: measurements taken by ships, measurements taken by satellites, and measurements taken by *drifters*, instrument packages that drift in the ocean and periodically relay data to satellites. Satellites can directly record data only from the oceans' surface, and drifters have been deployed only within the last decade, so historical data about the deep ocean comes primarily from ships. After quality

checks, all such data is eventually stored at the National Oceanographic Data Center, NODC (www.nodc.noaa.gov), where it is publically available.

This paper reports an analysis of data recorded over a small spatial region near Bermuda. A sufficiently small region was chosen so that we can safely ignore spatial variability. An analysis of data from a wide region of the Atlantic will appear elsewhere. Our purpose here is to introduce subjective likelihood and demonstrate proof-of-concept. A map of the data is in Figure 1; the data's temporal distribution is shown in Figure 2.

The i 'th data point \vec{y}_i is recorded at time t_i and consists of temperatures $\vec{y}_i = (y_{i1}, \dots, y_{in_i})$ measured at depths $\vec{d}_i = (d_{i1}, \dots, d_{in_i})$. (Other properties are also measured, but we do not report on them here.) The first depth is always sufficiently close to the surface so that (1) we can assume y_{i1} is approximately equal to the surface temperature and (2) we can take $d_{i1} = 0$ without serious error. Temperature as a function of depth is called a temperature *profile*. Figure 3 shows one such profile.

Generally speaking, the upper layer of the ocean, because it is vertically mixed, should have a uniform temperature, while the stratified layer should have a monotonically decreasing temperature. (Cold water is denser, so sinks.) Figure 3 is typical. Locating the bottom of the mixed layer is easy in

Bermuda

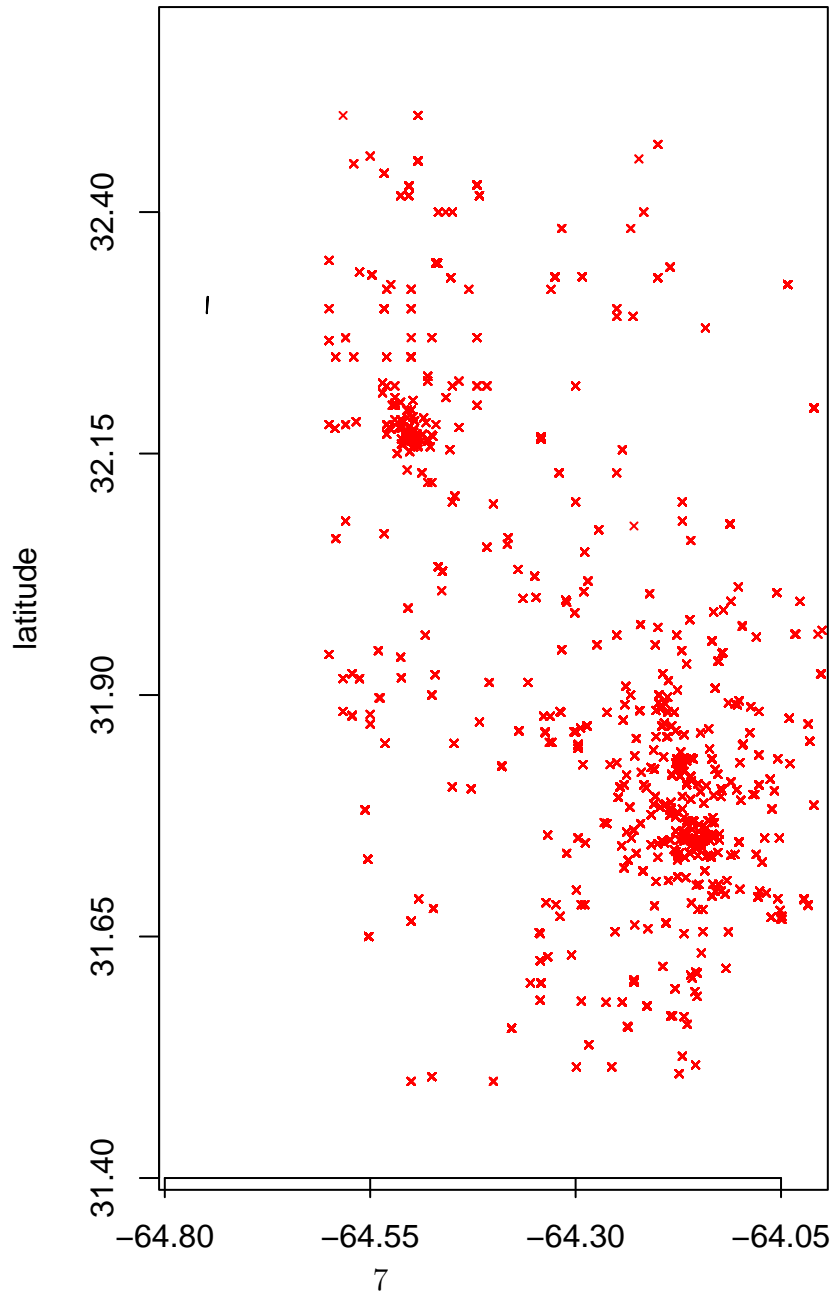


Figure 1: data locations near Bermuda

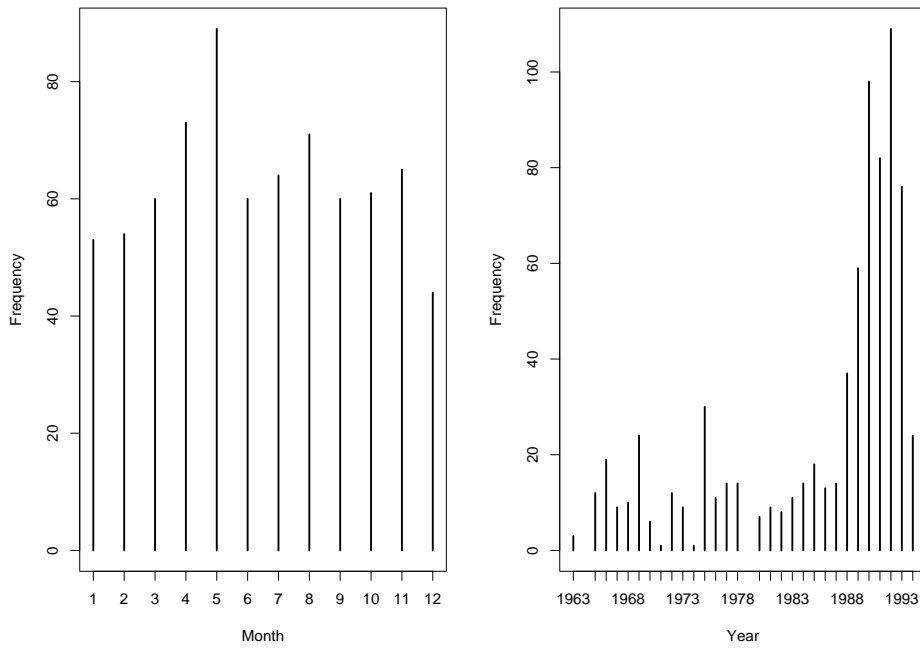


Figure 2: Sampling times near Bermuda

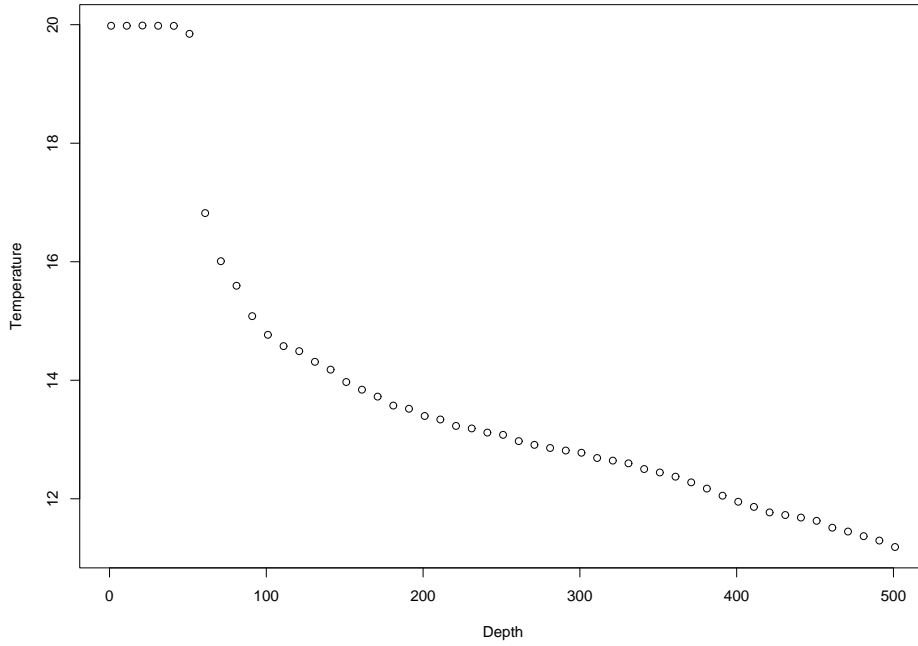


Figure 3: A nice profile: temperature as a function of depth measured at intervals of 10m. M appears to be between 40 and 60 meters.

such profiles. In Figure 3 we can say with confidence that M is somewhere near 50 meters.

First order physical considerations suggest that temperature should decrease exponentially from M to the ocean floor (Mellor [1996]), where it is about 2°C throughout the world. If that were true, then a change-point model with three parameters — surface temperature, M , and decay rate — would fit the data well. However, real data don't always exhibit exponential decay, as illustrated by Figure 4 which shows the same profile displayed in Figure 3 along with several exponential decay curves. In fact, real data don't always indicate M with much clarity. See, for example, Figure 5 which shows three profiles, none of which indicate M with much clarity.

4 Subjective Likelihood

4.1 Heuristic Explanation

In this section we consider what can be learned from a single profile \vec{y} sampled at depths \vec{d} ; the parameter of interest is M .

From either a likelihood or Bayesian perspective, what is needed is a sampling model $p(\vec{y} | M)$. But toward the end of Section 3 we used Figure 4

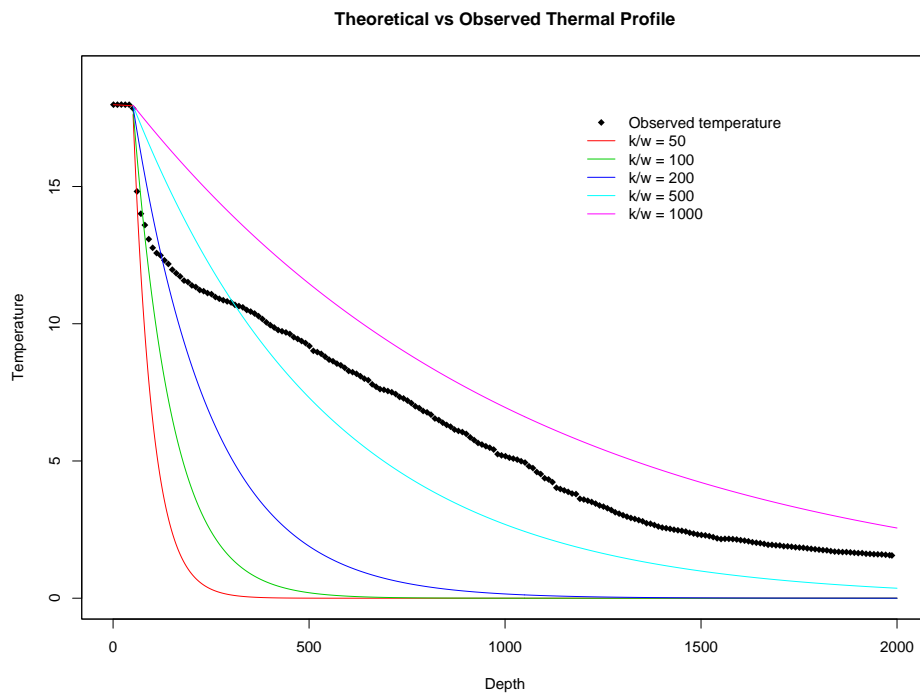


Figure 4: The same profile as in Figure 3 with several exponential decay curves. None fit the data well.

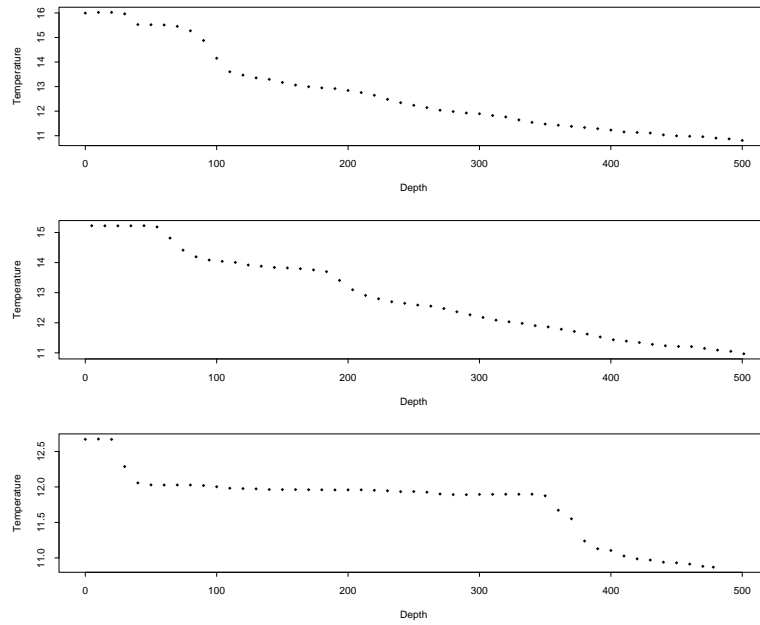


Figure 5: Three profiles. None indicate M with clarity.

to argue that the sampling model derived from first order physics doesn't fit the data. Further, our oceanographer Susan Lozier tells us that more detailed physical models are also unreliable. So how can we describe what is learned from \vec{y} ? We decided to ask the oceanographer directly.

We showed the oceanographer a profile (\vec{y}, \vec{d}) and asked what she could tell us about M , based on that profile. Her response was to tell us $\Pr[M \in I_j]$ for $j = 1, \dots, n$ where I_j is the interval from d_j to d_{j+1} . ($d_1 = 0$ is the ocean surface; d_{n+1} is the floor.) The process was repeated for several profiles, about a dozen. Figure 3 is an example. For this profile the oceanographer's assessments were

$$\Pr[M \in I_6] \approx 10 \Pr[M \in I_5]$$

$$\Pr[M \in \text{some other interval}] \approx \text{very small}$$

The next step was to ask the oceanographer how she makes her assessments. For an interval $I_j = [d_j, d_{j+1}]$ she considers two quantities: $y_1 - y_j$, the temperature drop from the surface to the top of I_j , and $(y_j - y_{j+1}) / (d_{j+1} - d_j)$, the rate of temperature drop within I_j . Small values of $y_1 - y_j$ and large values of $(y_j - y_{j+1}) / (d_{j+1} - d_j)$ imply that I_j is likely to contain M . She also says these are the only quantities that matter; other aspects of the profile

carry so little information as to be ignorable. To formalize, define

$$\vec{\Delta}_1 = (\Delta_{11}, \dots, \Delta_{1n}) = (0, y_1 - y_2, \dots, y_1 - y_n)$$

$$\vec{\Delta}_2 = (\Delta_{21}, \dots, \Delta_{2n}) = ((y_1 - y_2)/(d_2 - d_1), \dots, (y_n - y_1)/(d_{n+1} - d_n))$$

Then, according to the oceanographer, the probabilities $\Pr[M \in I_j]_{j=1}^n$ are some function $g(\vec{\Delta}_1, \vec{\Delta}_2)$.

After considering multiple profiles — some real and some artificially constructed to learn particular aspects of the oceanographer’s thinking — we settled on

$$\Pr[M \in I_j | \vec{y}, \vec{d}]_1^n \propto g(\vec{\Delta}_1, \vec{\Delta}_2) = \exp\{-2\vec{\Delta}_1\} \times [1 - \exp\{-\vec{\Delta}_2\}] \quad (2)$$

as providing sufficiently close approximation to the oceanographer’s posterior probabilities for the intervals I_j . (The left-hand side of (2) is a vector with one component for each interval. The right-hand side is also a vector; notation such as $\exp\{-2\vec{\Delta}_1\}$ means element-wise multiplication and exponentiation.)

Figures 6 and 7 show how Equation 2 works for the profiles in Figures 3 and 5. Unnormalized posterior probabilities calculated according to Equation 2 are plotted as horizontal bars over their respective intervals.

Two more facts are needed to complete the specification of the likelihood.

1. Because we did not tell the oceanographer the time of year or physical

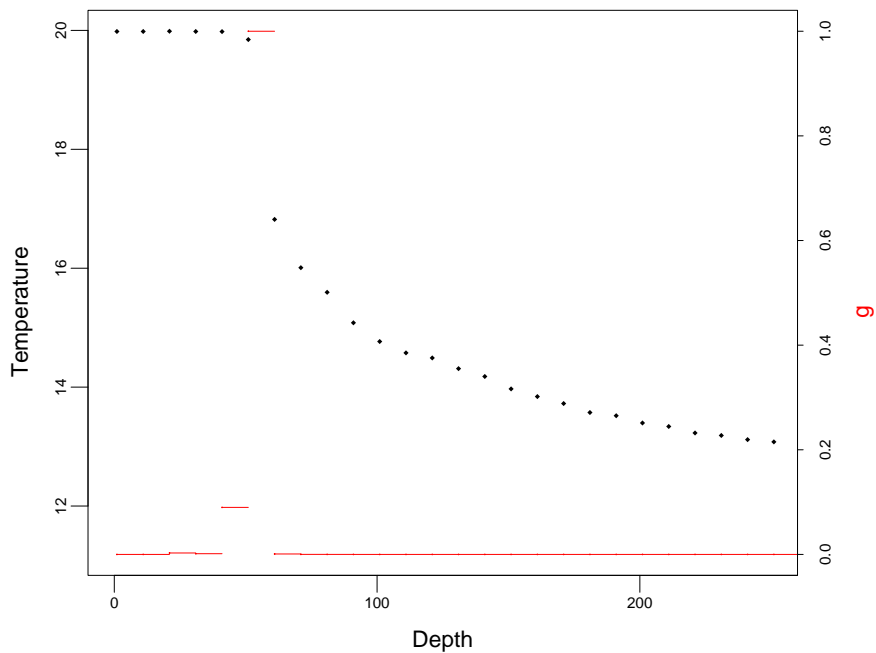


Figure 6: The profile of Figures 3 and 5. The horizontal bars show posterior probabilities of intervals calculated according to Equation 2, assuming a uniform prior. The bar over I_6 is approximately 10 times as high as the bar over I_5 . The oceanographer agrees that the horizontal bars approximately match her subjective evaluation.

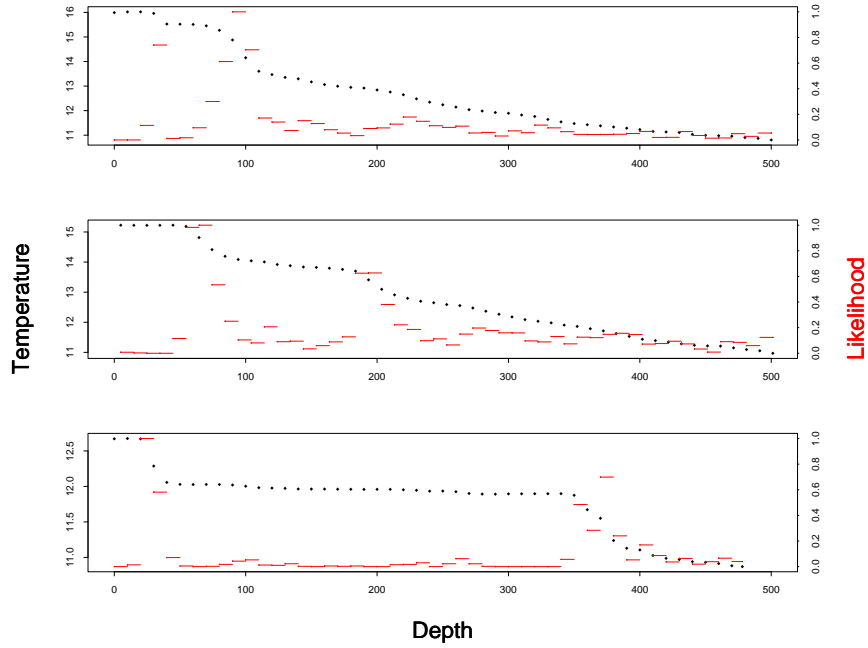


Figure 7: Three profiles. The horizontal bars show posterior probabilities of intervals calculated according to Equation 2, assuming a uniform prior. The oceanographer agrees that the horizontal bars approximately match her subjective evaluation.

location of the profiles, her prior for M was approximately uniform.

(She agrees.)

2. Her posterior for M is approximately uniform within each interval.

(She agrees.)

Equation 2 and Fact 2 specify the posterior density of M . It is piecewise constant on the intervals I_j ; its value on I_j is

$$p'(m | \vec{y}) = \frac{\exp\{-2\Delta_{1j}\} \times [1 - \exp\{-\Delta_{2j}\}]}{(d_{j+1} - d_j) \sum_k (\exp\{-2\Delta_{1k}\} \times [1 - \exp\{-\Delta_{2k}\}])} \quad (3)$$

for $m \in I_j$. And since the prior was uniform, Equation 3 is also the likelihood function.

One final consideration comes into play. Equation 2 was constructed to mimic the oceanographer's assessments of high probability intervals. For low probability intervals it accurately captures the fact that they have low probability, but might not accurately capture their probability ratios. The result could be that an analysis based on Equation 3 would be overly sensitive to "outliers", or intervals with low probabilities. So in consultation with the oceanographer we agree that the likelihood ratio $\ell(m)/\ell(\hat{m})$ should be bounded below by .01, where $\hat{m} = \operatorname{argmax} p'(m)$. We redefine the posterior

density as

$$p(m | \vec{y}) = \max[p'(m), .01p'(\hat{m})] \quad (4)$$

More formally, for any depth m let $j(m)$ be the interval containing m , i.e., $m \in I_{j(m)}$. Then we define the subjective likelihood function $\ell(m)$ by

$$\ell'(m) \propto \frac{\exp\{-2\Delta_{1j(m)}\} \times [1 - \exp\{-\Delta_{2j(m)}\}]}{d_{j(m)+1} - d_{j(m)}} \quad (5)$$

$$\ell(m) = \max[\ell'(m), .01\ell'(\hat{m})]$$

Equation 5 gives us a rule for computing the likelihood function for any profile. In subsequent sections we apply the rule to a large collection of profiles, more than the oceanographer can assess individually.

4.2 Semiformal Justification

Bayesian analysis derives from the joint distribution $p(\vec{y}, M)$. To arrive at $p(\vec{y}, M)$ one typically specifies $p(M)$ and $p(\vec{y} | M)$. Our analysis also uses $p(\vec{y}, M)$ but arrives at it differently.

Since the oceanographer cannot tell us directly about $p(\vec{y}, M)$ or $p(\vec{y} | M)$, but can tell us about the relationship between M and $(\vec{\Delta}_1, \vec{\Delta}_2)$, we work with a transformation of variables

$$(\vec{y}, M) \longleftrightarrow (M, \vec{\Delta}_1, \vec{\Delta}_2, \vec{s}),$$

find the joint distribution of $(M, \vec{\Delta}_1, \vec{\Delta}_2, \vec{s})$, and derive that of (\vec{y}, M) by back transformation. Specifically,

$$(y_1, \dots, y_n, m) \longleftrightarrow (m, \Delta_{1j(m)}, \Delta_{2j(m)}, s_1, \dots, s_{n-2})$$

where

$$s_k = \begin{cases} y_{d_k} - y_{d_{k-1}} & \text{for } k = 1, \dots, j(m) - 1, \\ y_{d_{k+2}} - y_{d_{k+3}} & \text{for } k = j(m), \dots, n - 2. \end{cases}$$

For later use, we note that for a fixed m this is a linear transformation and the absolute value of the Jacobian is $1/(d_{j(m)+1} - d_{j(m)})$. But the transformation and Jacobian vary according to $j(m)$.

The joint density of $(M, \vec{\Delta}_1, \vec{\Delta}_2, \vec{s})$ is given by

$$\begin{aligned} p(m, \Delta_{1j(m)}, \Delta_{2j(m)}, \vec{s}) &= p(m)p(\Delta_{1j(m)}, \Delta_{2j(m)} | m)p(\vec{s} | m, \Delta_{1j(m)}, \Delta_{2j(m)}) \\ &\approx p(m)p(\Delta_{1j(m)}, \Delta_{2j(m)})p(\vec{s}) \\ &\propto p(m)p(\Delta_{1j(m)}, \Delta_{2j(m)}) \\ &= p(\Delta_{1j(m)}, \Delta_{2j(m)}) \end{aligned}$$

The second line follows from the oceanographer's judgement that $M \perp (\vec{\Delta}_1, \vec{\Delta}_2)$ and $\vec{s} \perp (M, \vec{\Delta}_1, \vec{\Delta}_2)$, at least approximately. The third line follows because, while \vec{s} does depend on m — i.e., $\vec{s} = h(m, \vec{y})$ for some function h — the dependence of $p(\vec{s})$ on m is judged so slight as to be ignorable. The

term $p(\Delta_{1j(m)}, \Delta_{2j(m)})$ is retained because it does contain useful information about m . The fourth line follows because in this section $p(m) = 1$ in accord with the conditions of elicitation.

The oceanographer's judgment expressed in Equation 2 is equivalent to setting

$$\begin{aligned} p'(\Delta_{1j(m)}, \Delta_{2j(m)}) &\propto g(\Delta_{1j(m)}, \Delta_{2j(m)}) \\ &= \exp\{-2\Delta_{1j(m)}\} \times [1 - \exp\{-\Delta_{2j(m)}\}] \\ p(\Delta_{1j(m)}, \Delta_{2j(m)}) &= \max[p'(\Delta_{1j(m)}, \Delta_{2j(m)}), .01p'(\Delta_{1j(\hat{m})}, \Delta_{2j(\hat{m})})] \end{aligned}$$

The joint density of (\vec{y}, M) comes from the transformation

$$(M, \vec{\Delta}_1, \vec{\Delta}_2, \vec{s}) \rightarrow (\vec{y}, M).$$

Accounting for the Jacobian, it is

$$\begin{aligned} p'(\vec{y}, m) &\propto \frac{\exp\{-2\Delta_{1j(m)}\} \times [1 - \exp\{-\Delta_{2j(m)}\}]}{d_{j(m)+1} - d_{j(m)}} \\ p(\vec{y}, m) &\propto \max[p'(\vec{y}, m), .01p'(\vec{y}, \hat{m})] \end{aligned} \tag{6}$$

Since the prior was uniform, this is also the likelihood function, as heuristically justified in Equation 5.

Starting from Equation 6 one could, if one wished, try to derive $p(\vec{y} | m)$, the sampling model implied by our subjective elicitation exercise. In practice, since we already have $\ell(m)$, there is little need to do so.

5 Model and Prior

The observations $\vec{y}_1, \dots, \vec{y}_T$, shown in Figure 1, run over a time index $t = t_1, \dots, t_T$ that spans multiple years, as shown in Figure 2.

Figure 8 shows the result of applying Equation 2 to each profile separately. Each vertical bar is the maximum probability interval of some profile; its extent is indicated on the ordinate. Its abscissa is the day-of-year when that profile was recorded. (The curve is a posterior mean and will be discussed later.) There are two features of note. First, there is an annual cycle with deeper mixed layers in the winter. And second, there is greater variability in the winter. Our model will accomodate both features.

Let $M(t)$ be the mixed layer depth at time t . It is apparent that $M(t)$ undergoes an annual cycle, the precise details of which are unknown and may vary from year to year.

Mean annual cycle We use μ to denote the mean annual cycle. Thus for any time t ,

$$\mu(t) = \mu(t \bmod 365).$$

We model μ with a *process convolution* (See Higdon [1998] for details.), as described in the next paragraph.

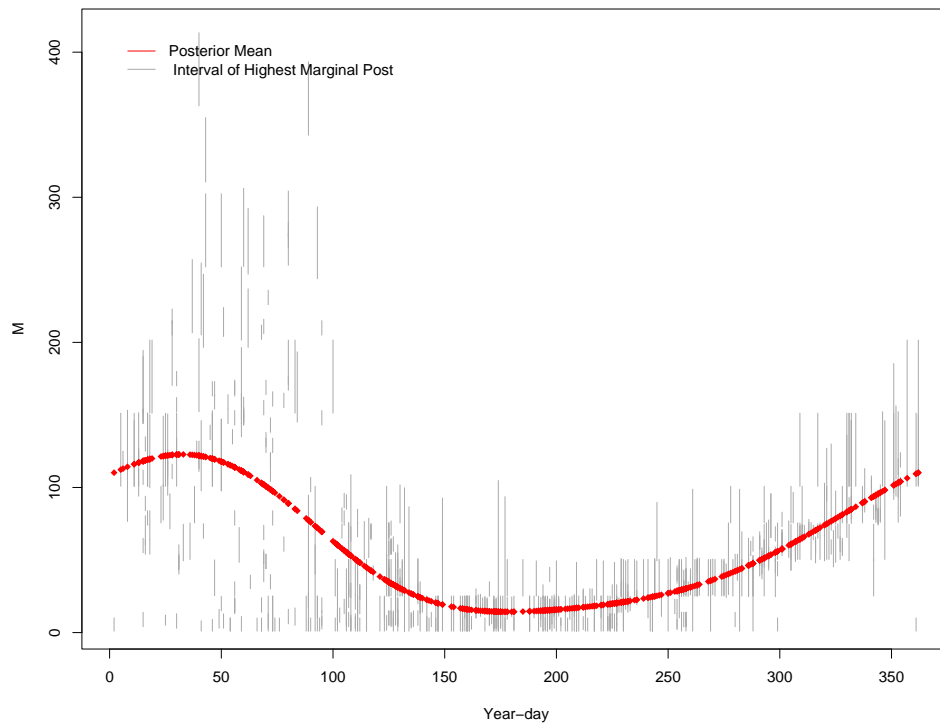


Figure 8: Vertical bars are maximum probability intervals of all profiles versus day-of-year. The curve is the posterior mean of $\mu(t)$.

Let $0 \leq v_1 < v_2 < \dots < v_{12} \leq 365$ be an equally spaced sequence of points (mod 365); let x_1, \dots, x_{12} , be values “at” those points; and let k be a kernel. Our model is

$$\mu(t) = \sum_{\ell=1}^{12} x_{\ell} k(t - v_{\ell})$$

The x_{ℓ} ’s are modelled as unknowns to be fit from the data. A priori,

$$x_1, \dots, x_{12} \sim \text{i.i.d. } \mathcal{N}(0, \sigma_x^2)$$

The posterior means of the x_{ℓ} ’s yields the estimate $\hat{\mu}(t) = \sum \hat{x}_{\ell} k(t - v_{\ell})$ plotted in Figure 8.

Deviations from μ The mixed layer deepens in the Fall as atmospheric temperatures decrease. Colder air means colder sea surface temperature, which in turn means that surface waters become dense and sink. The sinking causes surface waters to mix with deeper waters. The process continues through the winter, leading to deeper mixing and increased values of M . The effect is reversed in the Spring as surface waters warm. Spring heat is conveyed downward through diffusion, a much slower process than Fall’s convection. Thus the annual cycle is asymmetric and the summer mixed layer is relatively shallow and stable.

Because weather varies from year to year, the actual cycle for M in a

particular year may differ from μ , especially in the winter. To account for those differences we allow each winter month (November through April) to have its own random effect. Our notation for the random effect of month m in year y is $b_{y,m}$. Let $y(t)$ and $m(t)$ denote the year and month of time t , respectively.

In addition to annual variations due to weather, we are interested in a possible secular trend. We account for that in our model with a linear regression term βt . We will be interested in the posterior distribution of β .

Finally, to account for M 's greater variability in the winter than in the summer, we use a piecewise constant variance: σ^2 in the summer and $3\sigma^2$ in the winter. Modelling the variance as piecewise constant is crude but, we believe, effective.

Putting everything together, the full model and prior are

$$x_1, \dots, x_{12} \sim \text{i.i.d. } \mathbb{N}(0, \sigma_x^2)$$

$$\mu(t) = \sum_{\ell=1}^{12} x_\ell k(t - v_\ell)$$

$$\{b_{y,m}\} \sim \text{i.i.d. } \mathbb{N}(0, \sigma_b^2)$$

$$\beta \sim \mathbb{N}(0, \sigma_\beta^2)$$

$$\vec{x}, \vec{b}, \beta \text{ mutually independent}$$

(7)

$$\nu(t) = \mu(t) + b_{y(t),m(t)} + \beta t$$

$$\tau(t) = \begin{cases} \sigma^2 & \text{if } t \text{ is in winter} \\ 3\sigma^2 & \text{if } t \text{ is in summer} \end{cases}$$

$$M_{t_i} | \vec{x}, \vec{b}, \beta \sim \mathbb{N}(\nu(t_i), \tau(t_i)) \text{ mutually independent}$$

$$\vec{y} | \vec{x}, \vec{b}, \beta, \vec{M} \sim \text{subjective likelihood, mutually independent}$$

6 Computations and Posterior

The full conditional distributions are available for all parameters except the M_{t_i} 's. Therefore, one efficient method to sample from the posterior distribution is a Gibbs sampler with Metropolis-Hasting steps for the M_{t_i} 's.

Conditionally on current values of $\nu(t_i)$, we propose a new move $M_{t_i}^* \sim$

$\mathbb{U}[0, \text{ocean floor}]$ and accept the move with probability

$$\min \left\{ 1, \frac{\ell(M_{t_i}^*) \exp\left\{-\frac{(M_{t_i}^* - \nu(t_i))^2}{2\tau(t_i)^2}\right\}}{\ell(M_{t_i}) \exp\left\{-\frac{(M_{t_i} - \nu(t_i))^2}{2\tau(t_i)^2}\right\}} \right\}$$

where ℓ is the subjective likelihood function defined by Equation 5.

Figure 8 shows $\hat{\mu}(t) = \sum \hat{x}_\ell k(t - \nu_\ell)$, the estimate of μ calculated from the posterior means \hat{x}_ℓ . Note that it is asymmetric, as expected from our understanding of the physical process. The asymmetry is partial justification for modelling μ as a process convolution rather than a summation of sinusoids. Figure xyz shows several draws from the posterior distribution of μ , to give some idea of how well we can estimate the annual cycle. **[description here, once we see the plot.]** Figure 9 is another way to view the fit of the model. For each profile it shows the posterior mean of ν_i on the abscissa and the maximum probability interval according to Equation 2 on the ordinate. Figure 9 indicates an overall reasonably good fit and heteroscedasticity associated with the deeper mixed layers of winter. The x_ℓ 's themselves are not of interest, so we don't show any pictures.

Figure xyz shows the posterior densities of the $b_{y,m}$'s. One might ask whether the $b_{y,m}$'s from a given year are related. Figure abc shows the posterior means of the $b_{y,m}$'s from a given year joined together, so we can see the progression of random effects through the course of each year separately.

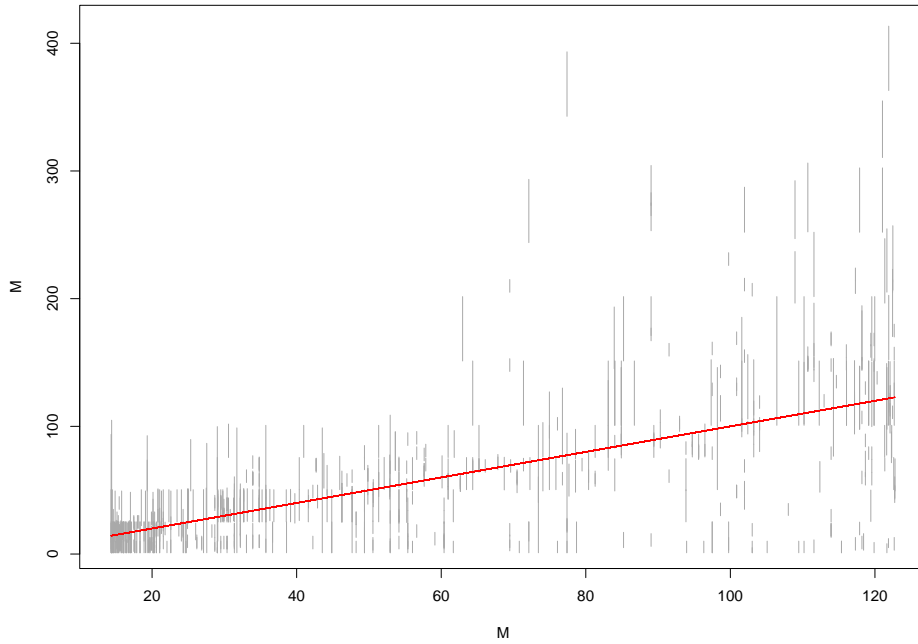


Figure 9: Maximum probability interval from Equation 2 vs. posterior mean of ν_i .

[description here, once we see the plot.]

One way to look for a secular trend is to fit a model identical to Equation 7 but without β and examine the random effects for evidence of trend. Figure 10 does just that; it shows the posterior mean $b_{y,m}$'s from such a fit. For each month they are plotted as a function of year. There is no evidence of trend except possibly for December. However, the apparent trend in December is due to confounding. December measurements in recent years tended to be early in the month, hence with shallower mixed layers and lower M 's, and therefore with negative $b_{y,m}$'s.

There is evidence of greater variability in the late winter since about 1990. We're not sure why that is, or even whether it's real.

Another way to look for a secular trend is to examine the posterior distribution of β . See Figure 11. Again, there is no evidence of trend.

7 Discussion

Foundations We like our subjective likelihood approach in this analysis because it incorporates expert judgment in the most direct way we can imagine. We find it an elegant and practical solution to a difficult modelling prob-

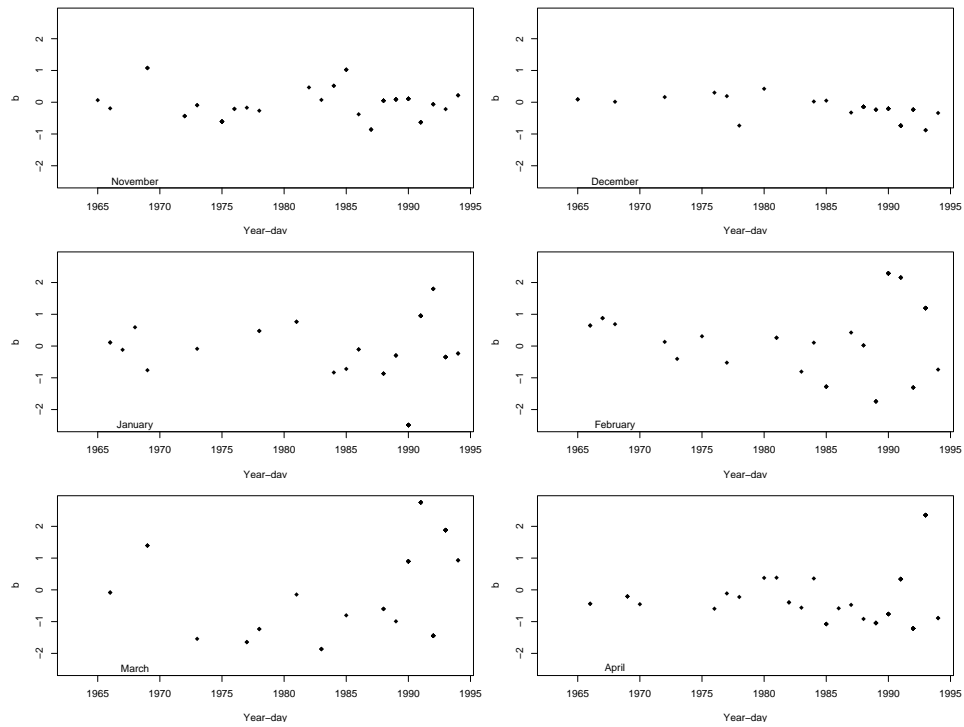


Figure 10: Random effects: $\beta_{y,m}$ vs. year

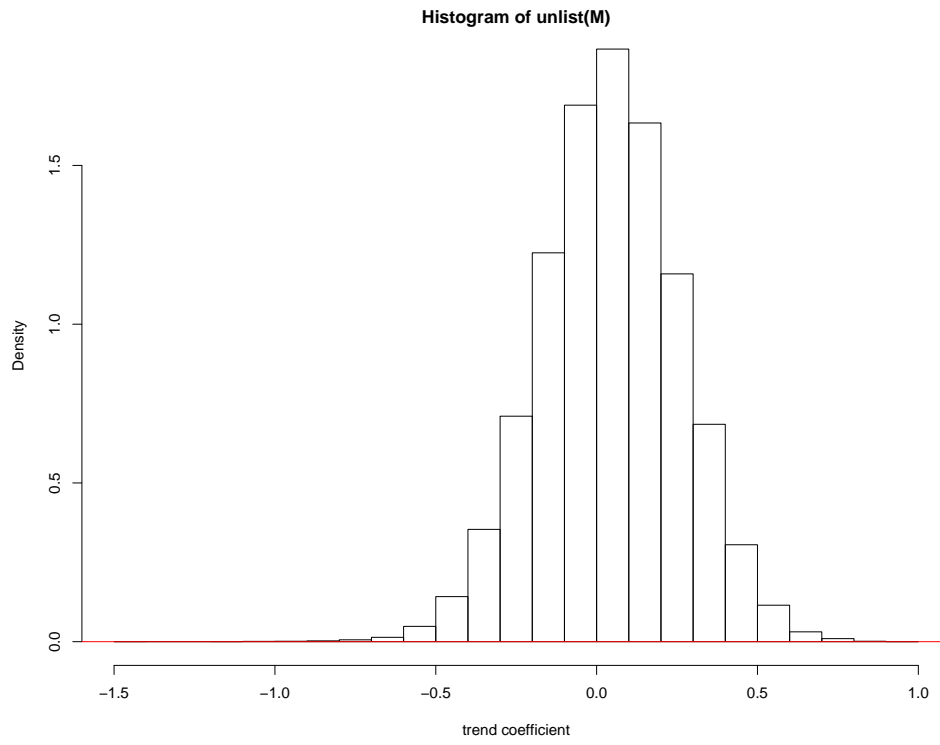


Figure 11: Posterior distribution of β : draws from the MCMC sampler.

lem. Of course, it does not have the usual philosophical underpinnings of the customary Bayesian analysis. Also it raises the question: if the oceanographer can give her posterior for M_{t_i} after seeing one profile, why can't she give her posterior for β after seeing them all? We think the answer is obvious. First, studying hundreds of profiles in detail (thousands when we analyze the entire Atlantic Ocean) is too difficult, and second, carefully assimilating information from all the profiles into an opinion about β is far removed from oceanographers' experience.

We could have analyzed the data with a nonparametric change-point model in which temperature is roughly constant down to a depth M , then decreases monotonically, but otherwise nonparametrically, to the ocean floor. We tried and rejected such an approach for two reasons. First, it yields results for single profiles that disagree with the expert's opinions, and second, it is a more circuitous use of expert opinion than the subjective likelihood function. Our nonparametric change-point model is described in the Appendix.

Will subjective likelihood be accepted by the scientific community; will there be other applications; will someone discover a fatal flaw? We don't know. We hope the answers are yes, yes, and no; but time will tell.

Modelling We made some fairly crude modelling choices. In particular, there are probably better and more sophisticated ways to handle random effects, heteroscedasticity, and the secular trend. We made our choices for simplicity and in the belief that more sophistication would not change the analysis very much. We acknowledge that improvements are possible.

Our model treats the profiles as conditionally independent given \vec{M} . That's a questionable choice. Our expert says that the time constant of the ocean, at least for this purpose, is about 5 days or so. Profiles taken on consecutive days are probably created and influenced by almost the same physical forces and are certainly dependent. Whether they are conditionally dependent given M is another matter. In any case, there are few profiles in our data set at time intervals of less than a week, so we are willing to treat them as conditionally independent. A possible model enhancement is to use a temporal covariance function with a range on the order of about 5 days.

Another way to improve the model is to include more covariates. M is related to air temperature, so one might try including covariates such as a running mean monthly temperature, etc. But temperature covariates will be highly correlated with time of year, so the potential for improved fit might be only minor. M is also thought to be related to El-Nino/La-Nina, so the

NAO (North Atlantic Oscillation) index might be a good covariate to try.

Diagnostics and Robustness Figures 8 and 9 show overall goodness of fit. Deviations from the fitted curves are a bit hard to interpret because the likelihood function is not symmetric and need not even be unimodal. For example, Figures 8 and 9 both show three profiles in which the interval of highest probability is deeper than 300m, yet the fitted value for one is around 80m and for the other two around 120m. The model appears not to fit those profiles well. What Figures 8 and 9 do not reveal is that each of those profiles has a secondary probability mode, according to Equation 2, so the apparent misfit is not so severe after all. Other profiles taken around the same dates as these three have only shallower modes; so the model favors the shallower modes in its posterior mean.

Determination of M can sometimes be complicated by daily warming of surface waters. During a hot, sunny day surface waters can warm as much as perhaps a couple of degrees down to a depth of perhaps 20m or so, then cool again during the night. Consequently, a profile taken in midafternoon might incorrectly indicate that M appears to be less than 20m. Our expert oceanographer was aware of this possibility when assessing the profiles we

showed her. The coefficient of Δ_1 in Equations 2 and 6, i.e. -2, reflects her belief that temperature drops in the upper ocean are probably due to mixed layers, not daily warming. But perhaps she's overly confident on this point. As a robustness check, we recalculated our posterior using a coefficient of -0.15. It made little difference to the inference regarding trend.

Our agreement that $\ell(m)/\ell(\hat{m}) \geq .01$ ensures that the posterior will not be too heavily influenced by a small number of profiles. Still, more thorough model diagnostics are useful and will be reported elsewhere.

8 Appendix

This Appendix briefly describes a nonparametric changepoint model as an alternative to the subjective likelihood analysis. In the end we prefer subjective likelihood because (1) it directly tackles the strength of evidence problem and (2), the changepoint model doesn't accurately capture the expert's posterior opinion. In this Appendix it suffices to consider a single profile at a single location in space and time.

We consider the profile, temperature as a function of depth, or $t(d)$, to be a realization of a random function. The function t is continuous, flat on $[0, M]$

and monotonically decreasing on $[M, \text{ocean floor}]$. If temperature is properly rescaled to the unit interval then t is a cdf, and we model it with a Dirichlet process. (See Lavine and Mockus [1995] for details of modelling monotone functions with Dirichlet processes.) We take M to be random, and the shape parameter of the Dirichlet process to be flat on $[0, M]$ and exponential on $[M, \text{ocean floor}]$, to agree with first order physical calculations. We tried three different values for the total mass parameter of the Dirichlet process, $\alpha = .005, .01, .1$. Finally, we model the observations as

$$y_i \sim \mathcal{N}(t(d_i), \sigma^2) \quad \text{mutually independent given } t$$

The posterior is calculated by MCMC. Figures 12 and 13 show results for two profiles. Figure 12 is the same profile shown in Figure 3; Figure 13 is the third profile in Figure 5. The curves in Figures 12 and 13 are posterior densities of M from the Dirichlet process changepoint model.

The expert's assessment of Figure 12 is that

$$\Pr[M \in I_6] \approx 10 \Pr[M \in I_5] \quad \text{and} \quad \Pr[M \notin I_5 \cup I_6] = \text{small}$$

But the Dirichlet process changepoint model gives most of its posterior mass to I_5 .

The expert's assessment of Figure 13 is bimodal; there are two likely

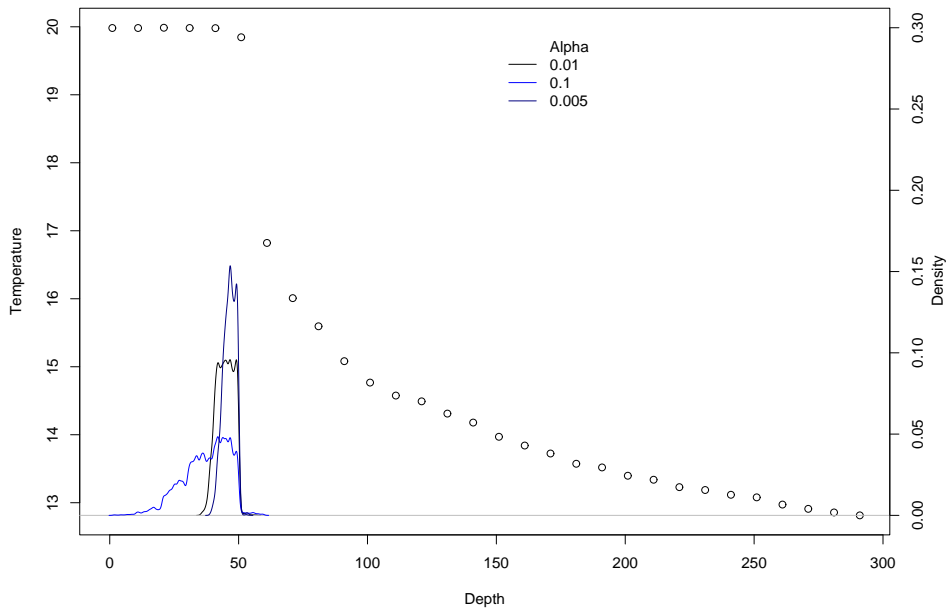


Figure 12: A profile and three posterior densities for M , according to the Dirichlet process changepoint model.

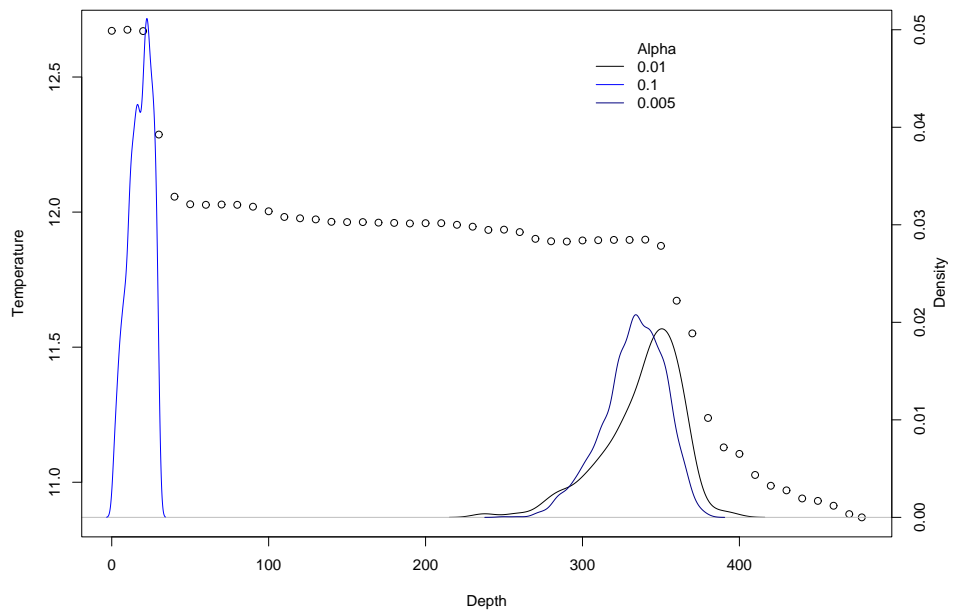


Figure 13: A profile and three posterior densities for M , according to the Dirichlet process changepoint model.

locations for M , one around 30m and one around 350m. However, as the figure shows, the Dirichlet process changepoint posterior for M is concentrated around one or the other of the two regions, but does not have two modes.

While it might be possible to refine the changepoint model to better reflect expert opinion, we are not sure how to go about it. Since the expert's opinion is about the posterior and not about the sampling model, we thought it more straightforward and justifiable to model that opinion directly through subjective likelihood rather than indirectly through a sampling model.

References

- N. L. Bindoff and T. J. McDougall. Diagnosing climate change and ocean ventilation using hydrographic data. *Journal of Physical Oceanography*, 24:1137–1152, 1994.
- David Higdon. A process-convolution approach to modelling temperatures in the north atlantic ocean. *Environmental and Ecological Statistics*, 5:173 – 190, 1998.
- M. Lavine and S. Lozier. A Markov random field spatiotemporal analysis

- of ocean temperature. *Environmental and Ecological Statistics*, 6:249–273, 1999.
- M. Lavine and A. Mockus. A nonparametric Bayes method for isotonic regression. *Journal of Statistical Planning and Inference*, 46:235–248, 1995.
- Sydney Levitus. Interpentadal variability of temperature and salinity at intermediate depths of the North Atlantic, 1970–1974 vs. 1955–1959. *J. Geophys. Res.*, 94:6091–6131, 1989a.
- Sydney Levitus. Interpentadal variability of temperature and salinity in the deep North Atlantic, 1970–1974 vs. 1955–1959. *J. Geophys. Res.*, 94:16125–16131, 1989b.
- G. L. Mellor. *Introduction to Physical Oceanography*. American Institute of Physics, Woodbury, New York, 1996.
- Gregorio Parrilla, Alicia Lavin, Harry Bryden, Maria García, and Robert Millard. Rising temperatures in the subtropical North Atlantic Ocean over the past 35 years. *Nature*, 369:48–51, 1994.
- J.F. Read and W.J. Gould. Cooling and freshening of the subpolar North Atlantic ocean since the 1960s. *Nature*, 360:55–57, 1992.

D. Roemmich and C. Wunsch. Apparent changes in the climatic state of the deep North Atlantic ocean. *Nature*, 307:447–450, 1984.